Eur. Phys. J. B **57**, 299–303 (2007)
DOI: 10.1140/epjb/e2007-00171-x

THE EUROPEAN PHYSICAL JOURNAL B

Tunable supercurrent in a parallel double quantum dot system

H. Pan[1,a] and T.H. Lin[2]

[1] Department of Physics, Beijing University of Aeronautics and Astronautics, Beijing 100083, P.R. China
[2] State Key Laboratory for Mesoscopic Physics and Department of Physics, Peking University, Beijing 100871, P.R. China

Received 10 November 2006 / Received in final form 23 April 2007
Published online 15 June 2007 –

Abstract. The supercurrent through an Aharonov-Bohm interferometer containing two parallel quantum dots connected with two superconductor leads is investigated theoretically. The possibility of controlling the supercurrent is explored by tuning the quantum dot energy levels and the total magnetic flux. By tuning the energy levels, both quantum dots can be in the on-resonance or off-resonance states, and thus the optimal modulation of the supercurrent can be achieved. The supercurrent sign does not change by simply varying the quantum dot energy levels. However, by tuning the magnetic flux, the supercurrent can oscillate from positive to negative, which results in the π-junction transition.

PACS. 74.45.+c Proximity effects; Andreev effect; SN and SNS junctions – 73.23.-b Electronic transport in mesoscopic systems – 73.63.Kv Quantum dots

1 Introduction

Recent advances in nanotechnology have attracted much attention to the quantum coherence phenomena in the resonant tunneling processes of the quantum dot (QD) systems in which electron can keep phase coherence [1]. In the past decade, one of the adopted methods to study the phase coherence of an electron through a QD was to measure the current versus the magnetic fluxes through an Aharonov-Bohm (AB) interferometer with one QD in one of its arms [2]. The observed magnetic oscillation of the current indicates coherent transport through the QD [3–8]. Recently, an open parallel double quantum dot (DQD) threaded by a magnetic flux has been realized in experiments, where the coherence of the electron remains [1,9,10]. As a controllable two-level system, the parallel DQD system becomes one of the promising candidates as a quantum bit in quantum computation based on solid-state devices [11–13]. On the other hand, the superconductor coupled mesoscopic hybrid systems have also attracted much attention in recent years because of both fundamental interest and potential applications for future nanoelectronics [14–17]. The Andreev reflection happens at the normal-metal/superconductor (N/S) interface [18], in which an incoming electron from normal side is reflected as a hole and a Cooper pair is transferred into the superconducting condensate.

One of the most intriguing experimental results on mesoscopic superconductivity is how to control the supercurrent through a S/QD/S Josephson junction [19]. Recently, the supercurrent flowing through the quantized single particle energy states of a quantum dot has been observed experimentally [20]. More recently, a superconducting quantum interference device with two QDs in its arms has been realized [22], where the two QD energy levels can be controlled by two lateral electrostatic gates. Thus the two QDs can be tuned in the on-resonance or off-resonance states by means of the gate voltages. The Josephson current through a double quantum dot system in the Kondo regime has also been studied theoretically [21], and the results show that the supercurrent depend distinctly on the ratio of the coupling strength between the double dots and the one between the dots and the leads. Motivated by these, tt is natural to ask if the DQD systems could have some novel phenomena associated with the supercurrent by tuning the two QD energy levels and the magnetic flux. In the work, we investigate how to control the supercurrent in a parallel DQD system by using the magnetic flux and the gate voltages. The scheme of the system is plotted in Figure 1. The device with the two quantum dots can be regarded as an AB interferometer threaded by magnetic fluxes. By using the nonequilibrium Green's function (NGF) techniques [23–25], we have analyzed quantum transport properties of the S/DQD/S system, which has some novel resonant features. The magnitude of the supercurrent can be controlled by tuning QD energy levels, which can lead to the on-resonance or off-resonance states of each QD. The sign of the supercurrent does not change by simply varying the QD energy levels. However, by tuning the magnetic fluxes, the supercurrent can oscillate from positive to negative. Whether the sign of the supercurrent changes depends not only on

[a] e-mail: hpan@buaa.edu.cn

$$\mathbf{\Sigma}^r_\alpha(\epsilon) = -\frac{i}{2}\rho(\epsilon)\begin{pmatrix} \Gamma_1^\alpha & -\Gamma_1^\alpha e^{i\phi_\alpha/2}\frac{\Delta}{\epsilon}e^{-i\varphi_\alpha} & \sqrt{\Gamma_1^\alpha\Gamma_2^\alpha}e^{i\phi_\alpha/2} & -\sqrt{\Gamma_1^\alpha\Gamma_2^\alpha}\frac{\Delta}{\epsilon}e^{-i\varphi_\alpha} \\ -\Gamma_1^\alpha e^{-i\phi_\alpha/2}\frac{\Delta}{\epsilon}e^{i\varphi_\alpha} & \Gamma_1^\alpha & -\sqrt{\Gamma_1^\alpha\Gamma_2^\alpha}\frac{\Delta}{\epsilon}e^{i\varphi_\alpha} & \sqrt{\Gamma_1^\alpha\Gamma_2^\alpha}e^{-i\phi_\alpha/2} \\ \sqrt{\Gamma_1^\alpha\Gamma_2^\alpha}e^{-i\phi_\alpha/2} & -\sqrt{\Gamma_1^\alpha\Gamma_2^\alpha}\frac{\Delta}{\epsilon}e^{-i\varphi_\alpha} & \Gamma_2^\alpha & -\Gamma_2^\alpha e^{-i\phi_\alpha/2}\frac{\Delta}{\epsilon}e^{-i\varphi_\alpha} \\ -\sqrt{\Gamma_1^\alpha\Gamma_2^\alpha}\frac{\Delta}{\epsilon}e^{i\varphi_\alpha} & \sqrt{\Gamma_1^\alpha\Gamma_2^\alpha}e^{i\phi_\alpha/2} & -\Gamma_2^\alpha e^{i\phi_\alpha/2}\frac{\Delta}{\epsilon}e^{i\varphi_\alpha} & \Gamma_2^\alpha \end{pmatrix}, \quad (7)$$

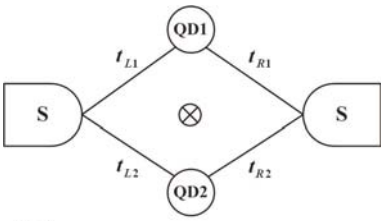

Fig. 1. Schematic diagram for a parallel DQD system connected with two superconducting leads.

the magnetic flux but also on QD energy levels. Therefore, the typical Josephson relation between the supercurrent and the macroscopic phase difference between the superconductors usually given by $I = I_c \sin\varphi$ changes to $I = -I_c \sin\varphi = I_c \sin(\varphi + \pi)$ (I_c is the critical current). The reverse sign of the supercurrent is referred to as the π-junction transition.

The rest of this paper is organized as follows. In Section 2 we present the model and derive the formula of the the current I by using the NGF technique. In Section 3 The control of the supercurrent with the magnetic fluxes and the dot energy levels are discussed in detail. Finally, a brief summary is given in Section 4.

2 Physical model and formula

The S/DQD/S system under consideration can be described by the following Hamiltonian

$$H = \sum_{\alpha=L,R} H_\alpha + H_D + H_T. \quad (1)$$

The H_α ($\alpha = L/R$) is the standard BCS Hamiltonian for the superconducting leads with the superconducting phase φ_α and the energy gap Δ,

$$H_\alpha = \sum_{k,\sigma} \epsilon_{\alpha,k} a^\dagger_{\alpha,k\sigma} a_{\alpha,k\sigma} + \sum_k [\Delta e^{-i\varphi_\alpha} a^\dagger_{\alpha,k\uparrow} a^\dagger_{\alpha,-k\downarrow} + H.c.], \quad (2)$$

where $a^\dagger_{\alpha,k\sigma}$ ($a_{\alpha,k\sigma}$) is the creation (annihilation) operators of the electron in the αth lead with energy $\epsilon_{\alpha,k}$. The chemical potential of the left and right leads are set as $\mu_L = \mu_R = 0$. H_D models the parallel double quantum dots as

$$H_D = \sum_{\sigma,i=1,2} (\varepsilon_i - V_{gi}) d^\dagger_{i\sigma} d_{i\sigma}, \quad (3)$$

where $d^\dagger_{i\sigma}$ ($d_{i\sigma}$) represents the creation (annihilation) operator of the electron with energy ε_i in the dot i ($i = 1, 2$). The energy levels in the dots are measured from the Fermi energy ($E_F = 0$) of the DQD system. H_T, which represents the tunneling coupling between the DQD and leads, can be expressed as

$$H_T = \sum_{\alpha,k\sigma,i=1,2} (t_{\alpha i} a^\dagger_{\alpha,k\sigma} d_{i\sigma} + H.c.), \quad (4)$$

where the tunneling matrix element $t_{L1} = |t_{L1}|e^{i\phi/4}$, $t_{L2} = |t_{L2}|e^{-i\phi/4}$, $t_{R1} = |t_{R1}|e^{-i\phi/4}$, and $t_{R2} = |t_{R2}|e^{i\phi/4}$. The phase due to the total magnetic flux threading into the AB ring is assumed to be $2\pi\phi/\phi_0$ with the flux quantum $\phi_0 = hc/e$.

The supercurrent can be calculated from standard NGF techniques, and can be expressed in terms of the dots Green functions as

$$I_\alpha(t) = \frac{2e}{\hbar} Re \int dt_1 Tr\{\hat{\sigma}_z[\mathbf{G}^<(t,t_1)\mathbf{\Sigma}^a_\alpha(t_1,t) + \mathbf{G}^r(t,t_1)\mathbf{\Sigma}^<_\alpha(t_1,t)]\}, \quad (5)$$

where $\hat{\sigma}_z$ is a 4×4 matrix with Pauli matrix σ_z as its diagonal components. The 4×4 Nambu representation is used to include the physics of Andreev reflection. The retarded and lesser Green's function are defined as $\mathbf{G}^r(t,t') = -i\theta(t-t')\langle\{\Psi(t), \Psi^\dagger(t')\}\rangle$ and $\mathbf{G}^<(t,t') = i\langle\Psi^\dagger(t')\Psi(t)\rangle$, respectively, with the operator $\Psi = (d^\dagger_{1\uparrow}, d_{1\downarrow}, d^\dagger_{2\downarrow}, d_{2\uparrow})^\dagger$. Let $\mathbf{g}^r(\epsilon)$ and $\mathbf{G}^r(\epsilon)$ denote the Fourier-transformed retarded Green's function of the QD without and with the coupling to the leads. In the Nambu representation, $\mathbf{g^r}(\epsilon)$ can be written as

$$[\mathbf{g}^r(\epsilon)]^{-1} = \begin{pmatrix} \epsilon-\varepsilon_1+i0^+ & 0 & 0 & 0 \\ 0 & \epsilon+\varepsilon_1+i0^+ & 0 & 0 \\ 0 & 0 & \epsilon-\varepsilon_2+i0^+ & 0 \\ 0 & 0 & 0 & \epsilon+\varepsilon_2+i0^+ \end{pmatrix}. \quad (6)$$

The retarded self-energy under the wide-bandwidth approximation is derived as

see equation (7) above.

where $\phi_L = -\phi_R = \phi$, and Γ^α_i ($i = 1, 2$) is the linewidth function describing the coupling between the dot and the αth superconducting lead. Under the wide-bandwidth approximation, the linewidth functions are independent on the energy variable. Furthermore, we set $\varphi_L = -\varphi_R = \varphi/2$ for the symmetric case. The factor $\rho(\epsilon)$ in the self energies is defined as

$$\rho(\epsilon) = \begin{cases} \frac{|\epsilon|}{\sqrt{(\epsilon^2-\Delta^2)}} & |\epsilon| > \Delta \\ \frac{\epsilon}{i\sqrt{(\Delta^2-\epsilon^2)}} & |\epsilon| < \Delta. \end{cases} \quad (8)$$

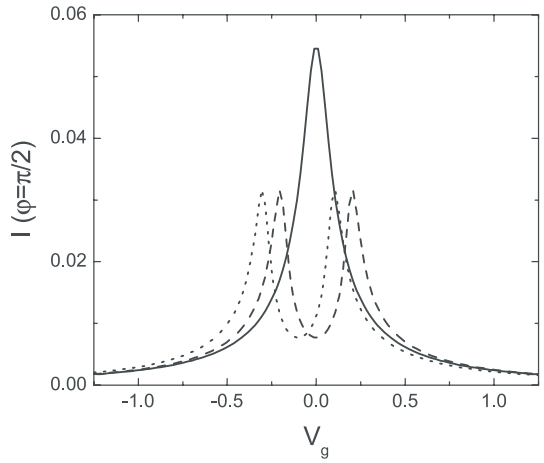

Fig. 2. Supercurrent $I(\varphi = \pi/2)$ vs. gate voltage V_g at $\phi = 0$ for various dot levels $\varepsilon_1 = \varepsilon_2 = 0$ (solid line), $\varepsilon_1 = 0.2, \varepsilon_2 = -0.2$ (dashed line), and $\varepsilon_1 = 0.1, \varepsilon_2 = -0.3$ (dotted line).

By using the Dyson equation, the retarded Green function of the system can be obtained as

$$\mathbf{G}^r(\epsilon) = \frac{1}{[\mathbf{g}^r(\epsilon)]^{-1} - \mathbf{\Sigma}^r(\epsilon)}, \tag{9}$$

where $\mathbf{\Sigma}^r = \mathbf{\Sigma}^r_L + \mathbf{\Sigma}^r_R$. After taking the Fourier transformation, the current formula becomes

$$I_\alpha = \frac{2e}{\hbar}\int \frac{d\epsilon}{2\pi} Tr\{\hat{\sigma}_z Re[\mathbf{G}^<(\epsilon)\mathbf{\Sigma}^a_\alpha(\epsilon) + \mathbf{G}^r(\epsilon)\mathbf{\Sigma}^<_\alpha(\epsilon]\}, \tag{10}$$

in the steady transport, the current is given by the following expressions

$$I = \frac{1}{2}(I_L - I_R) = \frac{e}{\hbar}\int \frac{d\epsilon}{2\pi} Tr\{\hat{\sigma}_z Re[\mathbf{G}(\mathbf{\Sigma}_L - \mathbf{\Sigma}_R)]^<\}. \tag{11}$$

Applying the fluctuation-dissipation theorem, one has

$$\mathbf{G}^<(\epsilon) = f(\epsilon)(\mathbf{G}^a(\epsilon) - \mathbf{G}^r(\epsilon)), \quad \mathbf{\Sigma}^<_{L/R} = f(\epsilon)(\mathbf{\Sigma}^a_{L/R} - \mathbf{\Sigma}^r_{L/R}), \tag{12}$$

where $f(\epsilon) = 1/(e^{\epsilon/k_BT}+1)$ is the Fermi distribution function. Consequently, the Josephson current is expressed as

$$\begin{aligned} I = & \frac{e}{\hbar}\int \frac{d\epsilon}{2\pi} f(\epsilon) Tr\{\hat{\sigma}_z Re[\mathbf{G}^a(\mathbf{\Sigma}^a_L - \mathbf{\Sigma}^a_R) \\ & - \mathbf{G}^r(\mathbf{\Sigma}^r_L - \mathbf{\Sigma}^r_R)]\}. \end{aligned} \tag{13}$$

The supercurrent originates from Andreev reflection at the interface between the superconducting leads and the central region. In the following section, the numerical results of the supercurrent and its dependence on the dot energy levels, magnetic flux, and the gate voltage are discussed in detail. We perform the calculations at zero temperature in units of $\hbar = e = 1$. The energy gap of the superconductor is fixed as $\Delta = 1$. All the energy quantities in the calculations are scaled by Δ.

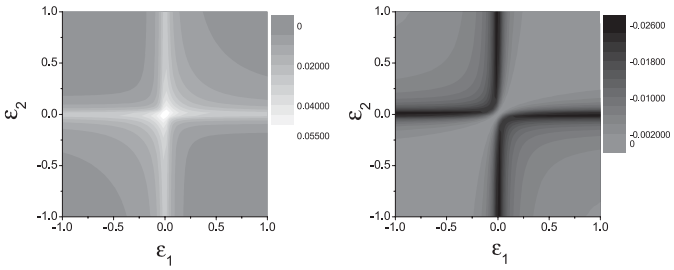

Fig. 3. The images of supercurrent $I(\varphi = \pi/2)$ as a function of the dots levels ε_1 and ε_2 with (a) $\phi = 0$ and (b) $\phi = \pi$.

3 Numerical results and discussions

For simplicity, we set $\Gamma^L_1 = \Gamma^L_2 = \Gamma^R_1 = \Gamma^R_2 = \Gamma$ with small values 0.05 for the symmetric and weak-coupling case. The gate voltage V_g dependence of the supercurrent $I(\varphi = \pi/2)$ with various quantum dot energy levels $(\varepsilon_1, \varepsilon_2)$ is shown in Figure 2. For the case of $(0, 0)$, there is only one current peak associated to the energy level $\varepsilon_1 = \varepsilon_2$ of the DQD. For the cases of $(0.2, -0.2)$ and $(0.1, -0.3)$, there are two current peaks associated to the two different energy levels ε_1 or ε_2 of the DQD, respectively. When the level ε_i is aligned with the Fermi energy, the supercurrent can flow by resonant tunnelling through the ith QD. When ε_i is far from the Fermi energy, the supercurrent is strongly reduced. The positions of the two peaks are symmetrical about the Fermi energy for $(0.2, -0.2)$, but they are not symmetrical for $(0.1, -0.3)$. The height of the current peak for $(0, 0)$ is about two times large as those for $(0.2, -0.2)$ and $(0.1, -0.3)$, since the two energy levels with the same values both contribute to the supercurrent.

The positions of the energy levels ε_1 and ε_2 can be tuned by the gate voltages. Figure 3 shows the images of the supercurrent $I(\varphi = \pi/2)$ as a function of ε_1 and ε_2. The bright regions correspond to positive current and the black regions to negative current. At zero magnetic flux $\phi = 0$, tuning the levels of the dots influences the the magnitude of the supercurrent significantly, but leaves the current sign unchanged. The current is symmetrical about the line of $\varepsilon_1 = \varepsilon_2$ and $\varepsilon_1 = -\varepsilon_2$ in the diagram. Our results agree well with those obtained in the experiment [22]. There are three cases for I versus ε_1 and ε_2 as discussed in the experiment. In case I, the both QD energy levels are aligned to the Fermi energy (on-resonance) and maximal supercurrent can flow through the device. In cases II and III, one and two of the QD energy levels are tuned away from the Fermi energy (off-resonance), respectively. When $\varepsilon_1 = \varepsilon_2 = 0$ as in case I, the supercurrent has a maximum value, since both QD are in the on-resonance states. When only $\varepsilon_1 = 0$ or $\varepsilon_2 = 0$ as in case II, the supercurrent is two times smaller as in case I, since one QD is in the on-resonance state and the other is in the off-resonance state. When both ε_1 and ε_2 are away from 0 as in case III, the supercurrent is very small, sine both QDs are in the off-resonance states. At nonzero magnetic flux $\phi = \pi$, the supercurrent becomes negative. Some similar "anticrossing" occurs at $\varepsilon_1 = \varepsilon_2$ in the diagram of

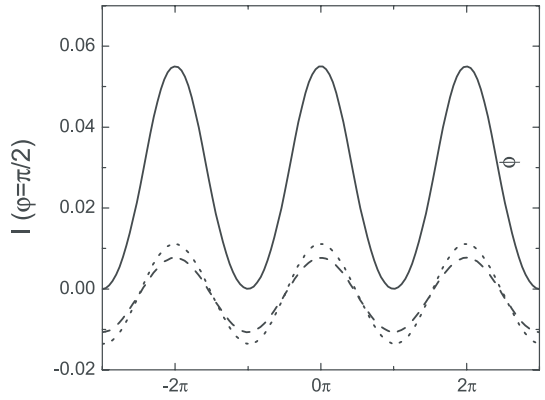

Fig. 4. The periodic oscillation of the supercurrent $I(\varphi = \pi/2)$ vs. the magnetic flux ϕ for dot levels $\varepsilon_1 = 0, \varepsilon_2 = 0$ (solid line), $\varepsilon_1 = 0.2, \varepsilon_2 = -0.2$ (dashed line), and $\varepsilon_1 = 0.1, \varepsilon_2 = -0.3$ (dotted line).

supercurrent. The QDs can be used as magnetic flux-controlled π-junctions, that is, the sign of the current-phase relation across the quantum dtos can be tuned with a magnetic flux.

We now discuss the AB oscillations of the supercurrent as a function of magnetic flux. In the hybrid system, the interfere channel paths contain two parts due to the Andreev reflection. One is the incident electron from the left superconductor lead to the right one, the other is the reflecting hole from the right superconductor lead to the left one. This leads to AB oscillations for the supercurrent. Figure 4 presents the dependence of the $I(\varphi = \pi/2)$ on the magnetic flux ϕ for various dots energy levels $(\varepsilon_1, \varepsilon_2)$. The energy levels of the DQD has a distinct influence on both the magnitude and the sign of supercurrent. The oscillation period of the supercurrent versus magnetic flux is 2π. Although the supercurrent for $(0, 0)$ oscillates with ϕ, it is always positive and does not change its sign. While for the cases of $(0.2, -0.2)$ and $(0.1, -0.3)$, not only the magnitude but also the sign oscillates with ϕ. The supercurrent sign changes from positive to negative, which is quite different from that for $(0, 0)$. At $\phi = 0$, the supercurrent for $(0, 0)$ is much larger than that for $(0.2, -0.2)$ and $(0.1, -0.3)$, since both quantum dots are in the on-resonance states. Compared with the results for the coupled two quantum dots in the Knodo regime [21], it is found that tuning the coupling strength only changes the amplitude of the supercurrent but leaves the sign of the supercurrent unchanged. However, both the amplitude and the sign of the supercurrent can be changed by tuning the magnetic flux. This characteristic transport features can be easily manipulated by applied gate voltages and magnetic flux.

The magnetic flux ϕ has an important influence not only on the magnitude but also on the sign of the supercurrent. As can be seen from Figure 5, the supercurrent I versus φ at $\phi = 0$ (solid line) and $\phi = \pi$ (dashed line) are quite different. For the case of $(0, 0)$, I oscillate with increasing φ and the period is 2π at $\phi = 0$, while I is always zero with increasing φ at $\phi = \pi$. For the case of $(0.1, -0.3)$,

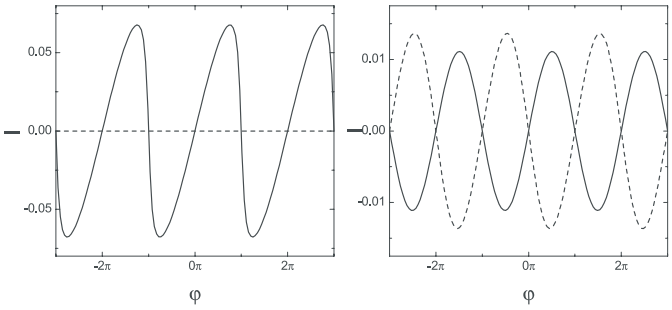

Fig. 5. The periodic oscillation of the supercurrent I vs. superconducting phase φ for dot levels (a) $\varepsilon_1 = 0, \varepsilon_2 = 0$, and (b) $\varepsilon_1 = 0.1, \varepsilon_2 = -0.3$ at $\phi = 0$ (solid line) and $\phi = \pi$ (dashed line).

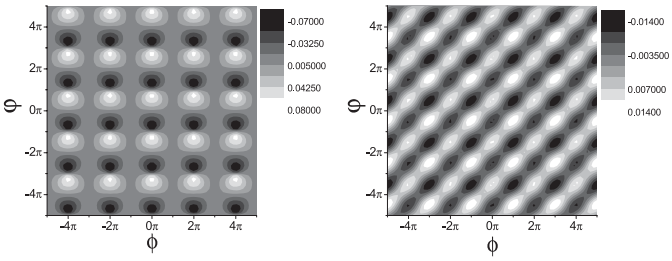

Fig. 6. The images of supercurrent I as a function of the superconducting phase φ and magnetic flux ϕ for dot levels (a) $\varepsilon_1 = 0, \varepsilon_2 = 0$, and (b) $\varepsilon_1 = 0.1, \varepsilon_2 = -0.3$.

the period of I with φ is 2π at both $\phi = 0$ and $\phi = \pi$. The current-phase relation is a $I = I_c \sin(\varphi)$-like function when there is no magnetic fluxes. However, the current sign is changed from positive to negative by the magnetic flux $\phi = \pi$. The negative sign can be absorbed into the phase factor as $\sin(\varphi + \pi)$, which is referred to as the π-junction transition. The π-junction transition is confirmed by the phase shift between the oscillations for I versus φ at $\phi = 0$ (solid line) and at $\phi = \pi$ (dashed line). In Figure 6, the images of the supercurrent I versus the superconducting phase φ and magnetic flux ϕ are plotted. The superconducting phase φ and the magnetic phase ϕ together can lead a complex picture for the supercurrent. Compared these results with those in the recent experiment [22], the image of the supercurrent shows similar behaviors, since the AB interference can make the supercurrent amplitude oscillate from large to small value just as the QD changes from the on-resonance to the off-resonance state. Furthermore, tuning φ and ϕ changes not only the the magnitude but also the sign of the supercurrent. The bright regions correspond to positive current and the dark regions to negative current. The periods of supercurrent versus ϕ or φ are both 2π. This opens a way to control not only the magnitude and sign of the supercurrent.

4 Summary

In summary, we have studied the tunable supercurrent through an AB interferometer containing two parallel quantum dots in terms of the nonequilibrium Green's

function method. Several ways to control the supercurrent are proposed, including the quantum dot energy levels ε_1 and ε_2 and the total magnetic flux ϕ treading the ring. By tuning the energy levels, both quantum dots can be in the on-resonance or off-resonance states, and thus the optimal modulation of the supercurrent can be achieved. The sign of the supercurrent does not change by simply varying the quantum dot energy levels ε_1 and ε_2. However, the supercurrent can oscillate from positive to negative by tuning the magnetic flux when ε_1 and ε_2 are at different sides of the Fermi energy, which results in the π-junction transition. It means that whether the oscillations can reverse the supercurrent depends distinctly on the quantum dot energy levels. Therefore, transport signals can be manipulated by adjusting the quantum dot energy levels and the magnetic fluxes together.

This project was supported by NSFC under Grants No. 10547102.

References

1. L.P. Kouwenhoven, C.M. Markus, P.L. McEuen, S. Tarucha, R.M. Westervelt, N.S. Wingreen, in *Mesoscopic Electron Transport*, edited by L.L. Sohn, L.P. Kouwenhoven, G. Schon (Kluwer, Dordrecht, 1997), Vol. 345 of NATO Advanced Study Institute, Ser. E
2. Y. Aharonov, D. Bohm, Phys. Rev. **115**, 485 (1959)
3. A.W. Holleitner, R.H. Blick, A.K. Httel, K. Eberl, J.P. Kotthaus, Science **297**, 70 (2002)
4. E. Buks, R. Schuster, M. Heiblum, D. Mahalu, V. Umansky, Nature (London) **391**, 871 (1998)
5. W.G. van der Wiel, S. De Franceschi, T. Fujisawa, J.M. Elzerman, S. Tarucha, L.P. Kouwenhoven, Science **289**, 2105 (2000)
6. Y. Ji, M. Heiblum, D. Sprinzak, D. Mahalu, H. Shtrikman, Science **290**, 779 (2000)
7. K. Kobayashi, H. Aikawa, S. Katsumoto, Y. Iye, Phys. Rev. Lett. **88**, 256806 (2002)
8. W.G. van der Wiel, S. De Franceschi, J.M. Elzerman, T. Fujisawa, S. Tarucha, L.P. Kouwenhoven, Rev. Mod. Phys. **75**, 1 (2003)
9. A.G. Aronov, Yu.V. Shavin, Rev. Mod. Phys. **59**, 755 (1987)
10. J. Konig, Y. Gefen, Phys. Rev. B **65**, 045316 (2002); B. Kubala, J. Konig, Phys. Rev. B **65**, 245301 (2002)
11. D. Loss, D.P. DiVincenzo, Phys. Rev. A **57**, 120 (1998)
12. X. Hu, S. Das Sarma, Phys. Rev. A **61**, 062301 (2000)
13. H. Lu, R. Lu, B.-F. Zhu, Phys. Rev. B **71**, 235320 (2005)
14. D.C. Ralph, C.T. Black, M. Tinkham, Phys. Rev. Lett. **74**, 3241 (1995)
15. N. Knorr, M.A. Schneider, Lars Diekhoner, P. Wahl, K. Kern, Phys. Rev. Lett. **88**, 096804 (2002)
16. M.R. Buitelaar, T. Nussbaumer, C. Schönenberger, Phys. Rev. Lett. **89**, 256801 (2002)
17. H. Takayanagi, T. Akazaki, J. Nitta, Phys. Rev. Lett. **75**, 3533 (1995)
18. W.J. Beenakker, Rev. Mod. Phys. **69**, 731 (1997)
19. J.J.A. Baselmans, A.F. Morpurgo, B.J. van Wees, T.M. Klapwijk, Nature (London) **397**, 43 (1999)
20. P. Jarillo-Herrero, J.A. van Dam, L.P. Kouwenhoven, Nature (London) **439**, 953 (2006)
21. R. López, M.S. Choi, R. Aguado, Phys. Rev. B **75**, 045132 (2007)
22. J.P. Cleuziou, W. Wernsdorfer, V. Bouchiat, T. Ondarcuhu, M. Monthioux, Nature Nanotechnology **1**, 53 (2006)
23. J.C. Cuevas, A. Martin-Rodero, A.L. Yeyati, Phys. Rev. B **54**, 7366 (1996); A.L. Yeyati, J.C. Cuevas, A. Lopez-Davalos, A. Martin-Rodero, Phys. Rev. B **55**, R6137 (1999)
24. H. Pan, T.H. Lin, D. Yu, Eur. Phys. J. B **47**, 437 (2005)
25. Q.F. Sun, J. Wang, T.H. Lin, Phys. Rev. B **62**, 648 (2000); Q.F. Sun, H. Guo, J. Wang, Phys. Rev. B **65**, 075315 (2002)